Effect of Interaction Energies on the Adsorption of Glycine onto a Cu(110) Surface: a Monte Carlo Simulation

R.O. Uñac, A.M. Vidales and G. Zgrablich

Invited Contribution

Effect of Interaction Energies on the Adsorption of Glycine onto a Cu(110) Surface: a Monte Carlo Simulation

R.O. Uñac, A.M. Vidales and G. Zgrablich* *INFAP-CONICET, Departamento de Física, Universidad Nacional de San Luis, Ejército de los Andes 950, 5700 San Luis, Argentina.*

ABSTRACT: The purpose of the present work was to study the effect of the adsorbate–adsorbate interaction energy for the glycine/Cu(110) system using a Monte Carlo simulation in the grand canonical ensemble. The dependence of the surface pattern structures upon the temperature and diffusion rate was studied. For either reversible or irreversible adsorption, the results showed that it is possible to obtain condensed phases with a large degree of correlation for high diffusion rates and temperatures. Depending on the set of interaction energies for nearest- and next-nearest-neighbour molecules, these patterns form either hetero- or homo-chiral footprint domains.

The results obtained are qualitatively consistent with the experimental pattern observed by other authors and allow an interpretation of the different proposed theoretical models used to explain experimental data.

1. INTRODUCTION

Chirality is a symmetry property of many molecules existing in Nature (or results as a product of chemical synthesis) which appears in two enantiomeric forms, *R* and *S*, each being the non-superimposable mirror image of the other. This property may lead to different enantiomers of the same chiral molecule interacting in different ways with other chemical structures of some complexity, in particular with biological molecules. For this reason, the production of pure enantiomeric species has become an issue of great importance for the pharmaceutical industry (Rouhi 2004).

In recent years, chiral heterogeneous catalysis has received special attention as a convenient technique for the manufacture of enantiomerically pure compounds (Lee and Zaera 2006). One promising route for achieving this is to use chiral modifiers to endow enantioselective properties onto a metallic surface (Baiker and Blaser 1997). This modification of the surface may act selectively towards the adsorption of another chiral probe species in two ways: (a) through a *one-to-one mechanism*, either by the formation of a complex between an individual modifier molecule and the reactant or by the creation of a single selective site on one side of the modifier (Tungler *et al*. 1989; Baiker 1997; LeBlond *et al*. 1999; Bürgi and Baiker 2000; Kubota and Zaera 2001; Chu *et al*. 2003; Ma and Zaera 2005) and (b) through a *template mechanism*, in which the chiral modifier adsorbs forming a superstructure, while the template which contains void spaces acts selectively on the adsorption of one of the enantiomers of the probe chiral species through

symmetry effects (Raval 2001; Ortega Lorenzo *et al*. 1999; Humblot *et al*. 2004; Stacchiola *et al*. 2002, 2005; Romá *et al*. 2004; Lee and Zaera 2005).

The template mechanism seems particularly adept for systems such as Pd(111) modified by the pre-adsorption of 2-butanol (Stacchiola *et al*. 2002), Pt(111) modified by 2-methylbutanoic acid (Lee and Zaera 2006) and Pt(111) modified by 2-butanol (Lee and Zaera 2005). In all these studies, chiral propylene oxide was used as the probe molecule to measure the enantioselective characteristics of the template. However, an understanding at a molecular level of the enantioselective process in a template system is far from being attained (Romá *et al*. 2003, 2004; Szabelski 2004; Szabelski and Sholl 2007a,b; López *et al*. 2008). Some studies (Szabelski 2004; Szabelski and Sholl 2007a,b) have shown how enantioselectivity of a chiral species can arise on a substrate with a pattern of strong and weak adsorbing sites. This mechanism could certainly apply in many cases. However, there are other systems, especially those studied experimentally by Lee and Zaera (2005, 2006) and Stacchiola *et al*. (2002, 2005), where preferential adsorption of one of the enantiomers could not be due to a difference in the adsorption energy of different sites. In fact, in these experiments, chiral probe molecules B were adsorbed onto a surface with a template formed by the pre-adsorption of another chiral molecule A — say its *R*-enantiomer — in such a way that first B(*R*) was adsorbed to saturation, then the amount adsorbed was measured via thermal desorption, and finally B(*S*) was adsorbed to saturation and the amount adsorbed again measured via thermal desorption. The ratio between these amounts, B(*R*)/B(*S*), then gave the enantioselectivity of the *R*-template surface. Under these conditions, a difference in the adsorption energies of B(*R*) and B(*S*) would only affect the adsorption kinetics, but since both enantiomers were adsorbed to saturation there would not be any measurable enantioselectivity. Hence, in this kind of system some steric effect should be present leading to the large observed enantioselectivity.

This steric effect is probably closely related to the superstructure chiral species formed on metal single crystals, which sometimes present an "extended chirality" (Raval 2002; Humblot and Raval 2005), and this, in turn, should depend strongly on the *footprint* of the adsorbed chiral species (i.e. the geometric form of the set of adsorbing sites occupied by the adsorbed species, or the projection of the adsorbed species on the metallic surface) and on the interactions between the adsorbed species (Humblot and Raval 2005; Barlow *et al*. 2004, 2005). Determination of the footprint of many of these chiral species is often difficult using experimental techniques such as LEED and STM (Humblot *et al*. 2004; Barlow *et a*l. 2005), and very little is known about the intermolecular interactions between the adsorbed species. Hence, simulation studies of the structures that adsorbed chiral species may form for given footprints and with assumed interactions may be helpful in understanding the behaviour of such systems.

The aim of the present work was to study precisely through Monte Carlo simulations the properties governing the adsorption of glycine onto Cu(110) surfaces, a system which has been studied intensively from the experimental point of view (Humblot *et al*. 2004; Chen *et al*. 2002; Barlow and Raval 2003; Barlow *et al*. 1998; Kang *et al*. 2003; Efstathiou and Woodruff 2003), to determine the effects of footprints and interactions on the structure of the adsorbate. In Section 2 we present the model and simulation algorithm used in this work, while the results obtained are presented and discussed in Section 3. Finally, our conclusions are given in Section 4.

2. MODEL AND SIMULATION ALGORITHM

Equilibrium adsorption of polyatomic molecules onto solid surfaces, e.g. glycinate onto Cu(110), can be satisfactorily simulated through a lattice–gas model and a grand canonical Monte Carlo

technique (Szabelski and Sholl 2007b). As in previous work (Uñac *et al.* 2007a,b), the metallic surface exposed to a gas phase composed of a racemic mixture of glycine molecules is represented by a square lattice of equivalent adsorption sites. This description, which is only a rough approximation since the Cu(110) surface presents heterogeneity due to different adsorption sites, preserves the main characteristics which are relevant for the study of the conditions for the formation of ordered patterns. Periodic boundary conditions are employed in the simulations and the method includes movement (Szabelski and Sholl 2007b; Mao *et al.* 2002). Since glycine molecules are not chiral in the gaseous phase, it is not necessary therefore to take into account chirality properties before the occurrence of adsorption. Glycine molecules adsorb as glycinate species, adopting two different possible footprints on the surface. Both footprints consist of two O atoms and one N atom bonded to the Cu atoms of the surface. We will name these footprints as (a) right triangle, as sketched in Figure 1(a) — this consists of a central O atom with additional O and N atoms placed as nearest-neighbours at the corresponding vertices of a right triangle — and (b) left triangle, as sketched in Figure 1(b), which is the mirror image of the right triangle footprint. Both representations mimic the footprints proposed by current models in the literature (Humblot *et al.* 2004; Chen *et al.* 2002; Barlow and Raval 2003; Efstathiou and Woodruff 2003; Raval 2003; Toomes *et al.* 2003; Rankin and Sholl 2004). Each adsorbed atom occupies one site of the lattice. The sharing of sites is forbidden.

Nearest- and next-nearest-neighbour interactions between two given molecules are accounted for, taking as a reference the positions of the central O atoms of each interacting molecule. These interactions between two adsorbed species are global in nature and will depend on their chirality.

The simulation algorithm is basically as follows. The temperature and chemical potential are fixed at the desired values. With a given probability, we choose which process is going to happen, viz. adsorption or desorption. These probabilities may, of course, be modified as desired. The algorithm is modified slightly to include the possibility of diffusion of the adsorbed molecules. In this sense, once a trial adsorption is performed on the lattice, a finite number of diffusion trials are also attempted.

Specifically, in our algorithm, an adsorption step is carried out as follows. A lattice site on which the process will take place is chosen at random. If the site is empty, we choose with the same probability which footprint is going to be adsorbed (left or right triangle); otherwise, the adsorption trial ends. Once the triangle form is known, we look for an empty space to adsorb this footprint,
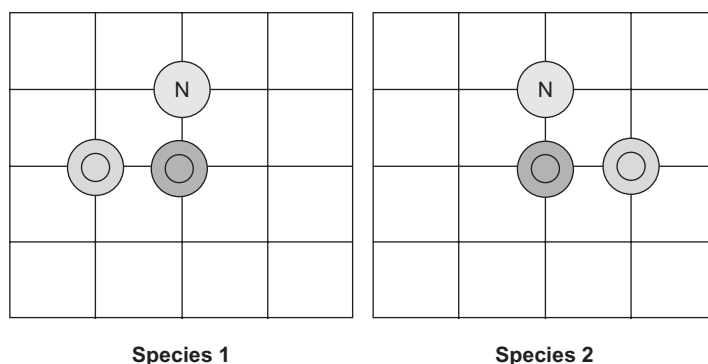
Species 1   **Species 2**

Figure 1. Schematic representation of the footprint motifs adopted by glycine molecules when they adsorb onto the Cu(110) surface. To the left is the representation of the named species 1 (right triangle) and, to the right, the corresponding representation for species 2 (left triangle).

i.e. if the corresponding neighbour sites are empty. Otherwise, the adsorption trial step is ended. If the whole cluster of sites is empty, adsorption is performed with the following probability:

$$P_{ads} = e^{-(\Delta E - \mu)/RT} \qquad (1)$$

where $\Delta E = E_f - E_0$; $\mu > 0$ is the chemical potential; $E = E_{ads} + W_{int}$, with W_{int} being the interaction energies between molecules. The quantity E_{ads} is always less than zero and here we use the same value for the two species. The situation $W < 0$ ($W > 0$) means an attractive (repulsive) interaction.

Irrespective of how the result of the adsorption step turns out, we perform N_{diff} trials for diffusion. In this case, a lattice site is chosen at random. If it is empty or if it is occupied by a non-central O atom, the trial fails. In the opposite case, we choose a random site among the first neighbours of the central O atom of the molecule. If the site is occupied, the trial ends; otherwise, we check for the cluster of empty sites necessary to complete the diffusion step. If this last condition is fulfilled, we accept diffusion based on the classical factor $\exp(-\Delta E/RT)$, where ΔE is the difference between the adsorption energies for the two configurations (Szabelski and Sholl 2007b).

If the selected process is desorption, the algorithm begins by choosing a lattice site on which the process will take place. If the site is empty or is occupied by a non-central O atom, the trial ends. Otherwise, desorption is performed with the probability:

$$P_{des} = e^{+(\Delta E - \mu)/RT} \qquad (2)$$

where ΔE is as defined above.

A given number of trials are performed until the final total coverage on the surface does not change by more than a small percentage — thus reaching a stationary condition. In general, after 5×10^5 trials, this equilibrium condition is fulfilled. It is worth mentioning, that even though the coverage does not change significantly, the pattern on the surface does change due to the effect of diffusion. For this reason, a large number of diffusion trials are performed (1×10^7) to find stationary patterns on the surface.

For the sake of completeness, in addition to the above adsorption–desorption equilibrium method, the process was also simulated as an irreversible random deposition process.

In our simulations, we employed the adsorption energies reported by Rankin and Sholl (2004) for the same system, i.e. $E_{ads} = 34.5$ kcal/mol, and we considered the same value for the two footprints. The value of μ was fixed at 5 kcal/mol. In this study, we consider the case of asymmetrical interactions between enantiomers and interaction energies of the order of 10% of the adsorption energies.

3. RESULTS AND DISCUSSION

Figure 2 depicts the results for low (a, b) and high (c, d) temperatures, with reversible adsorption in both cases. Bold symbols represent the central adsorbed oxygen atoms, grey ones belong to species 1 and black ones to species 2. Empty symbols represent the adjacent adsorbed atoms, O and N, forming the whole footprint. Grey and black correspond, as before, to species 1 and 2, respectively. For a better view of the patterns, we only show a part of the whole lattice.

For low temperature (300 K), the left snapshot [Figure 2(a)] corresponds to a set of interaction energies that are (i) zero for all nearest neighbours, (ii) attractive for next-nearest neighbours of the same species and (iii) repulsive for next-nearest neighbours of different species. This interaction energy configuration gives rise to homochiral domains for each species.
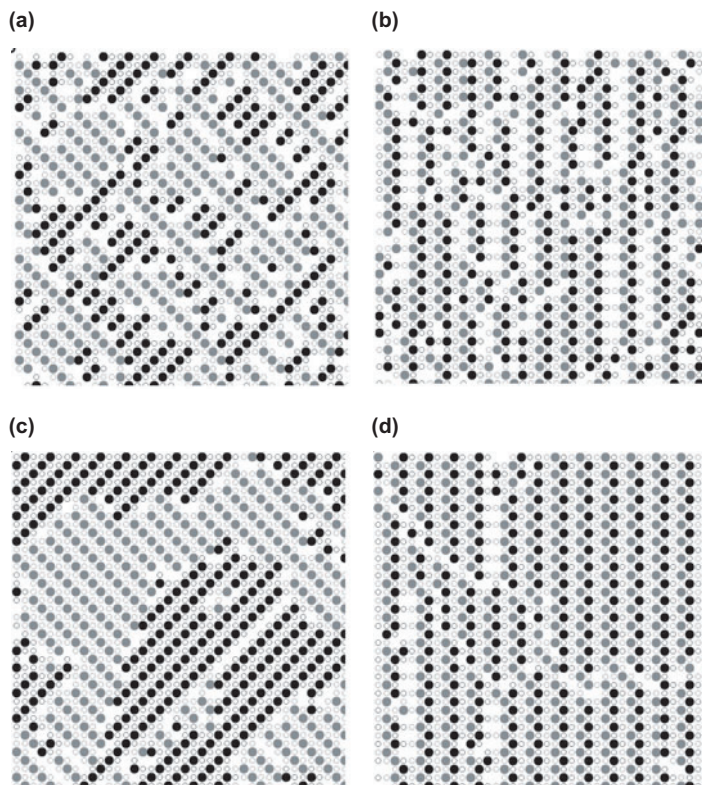
Figure 2. Snapshots of part of the simulated surface for glycine molecules reversibly adsorbed onto the Cu(110) surface. Adsorption energies are the same for the two species. (a) T = 300 K; $W_{22} = W_{11} = -5$ kcal/mol; $W_{21} = W_{12} = +5$ kcal/mol. W_{ij} represents the energy of interaction with next-nearest neighbours, where the index "i" represents one of the involved species and the index "j" corresponds to the other species involved in the interaction evaluation. (b) T = 300 K; $W_{22} = W_{11} = +5$ kcal/mol; $W_{21} = W_{12} = -5$ kcal/mol. (c) The same as for (a) but with T = 800 K. (d) The same as for (b) but with T = 800 K. MC steps = 5×10^5 and $N_{diff} = 1 \times 10^5$.

In contrast, the right snapshot [Figure 2(b)] corresponds to a heterochiral pattern and is obtained using a set of different interaction energies, viz. (i) zero for all nearest neighbours, (ii) repulsive for next-nearest neighbours of same species and (iii) attractive for next-nearest neighbours of different species.

For high temperature (800 K), Figures 2(c) and (d) correspond to the same set of energies as in Figures 2(a) and (b), respectively.

Two domains with different internal molecular arrangement may be identified, as observed in Figures 2(a) and (b). The organization of such domains depends upon the adsorbate–adsorbate interaction energies, giving rise to the growth of homochiral [part (a)] and heterochiral [part (b)] condensed patterns. Here, as in most literature on the subject (Barlow and Raval 2003), it is understood that a homochiral phase is considered as the collection of all adsorbed molecules with the same footprint (orientation) inside a given domain; and, conversely, a heterochiral domain is formed by molecules that adsorb with different alternative footprints.

Another feature of Figure 2(a) is the presence of two types of homochiral domains, each one with different biased orientation properly following their footprint local orientations. The transfer of the

footprint chiral character to the metallic surface has been observed both in simulations and experiments (Chen *et al.* 2002; Barlow and Raval 2003; Barlow *et al.* 1998; Efstathiou and Woodruff 2003; Uñac *et al.* 2007a,b). Nevertheless, to our knowledge, reported experiments for this system never refer to the presence of both homochiral orientations at the same time. On the other hand, only a single heterochiral domain is observed in Figure 2(b). The patterns shown so far resemble the observed ones discussed by Barlow and Raval (2003), but we never found the presence of both kinds of chiral domains *simultaneously* for a given set of the above-mentioned interaction energies.

In Figures 2(c) and (d), it is evident that the effect of increasing temperature favours the growth of the different domains. As the diffusion rate increases (due to increasing temperature), important condensate phase domains appear (either homochiral or heterochiral). This indicates that the diffusion mechanism is crucial to the formation of large highly correlated domains. It is important to note that our results mimic qualitatively those reported by other authors when temperature annealing is performed on a similar system (Barlow and Raval 2003; Barlow *et al.* 1998; Kang *et al.* 2003).

To ensure that the above results do not depend on conditions chosen as representing the steady state in our simulations, we performed the same set of simulations with an irreversible adsorption algorithm. The results obtained are shown in Figure 3, where the different snapshots correspond
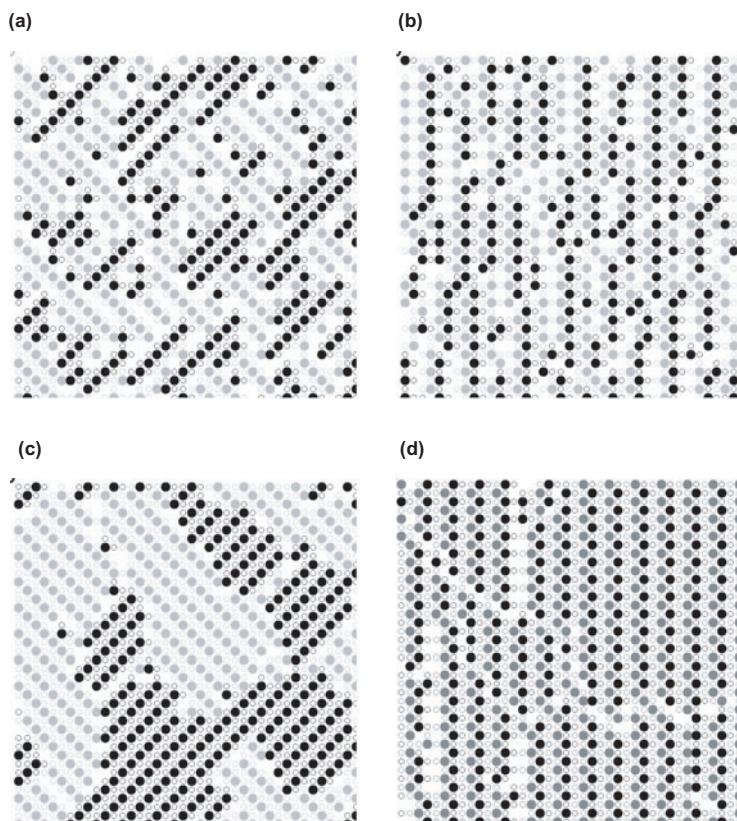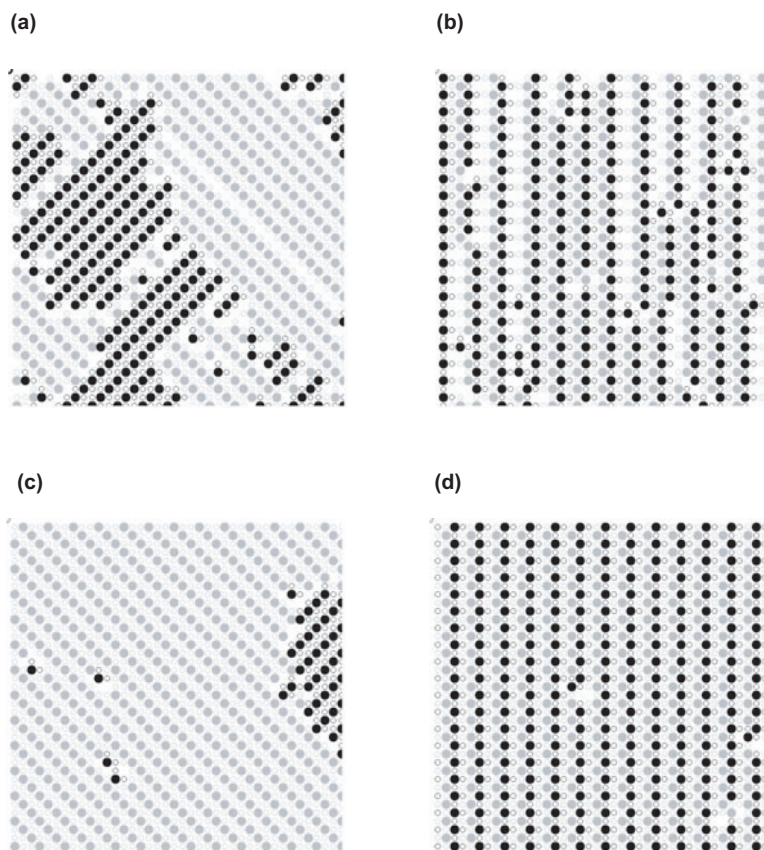

Figure 3. Snapshots of part of the simulated surface for glycine molecules irreversible adsorbed onto the Cu(110) surface. Adsorption energies are the same for the two species. (a) T = 300 K; $W_{22} = W_{11} = -5$ kcal/mol; $W_{21} = W_{12} = +5$ kcal/mol. (b) T = 300 K; $W_{22} = W_{11} = +5$ kcal/mol; $W_{21} = W_{12} = -5$ kcal/mol. (c) The same as for (a) but with T = 800 K. (d) The same as for (b) but with T = 800 K. MC steps = 5×10^5 and $N_{diff} = 1 \times 10^5$.

to the same cases as depicted in Figure 2. As can be seen, the patterns present the same qualitative characteristics as in Figure 2, thereby justifying the number of trial steps used in simulations to reach the stationary state. In addition, this last simulation protocol allows the inspection of the adsorption of chiral molecules that are tightly bound to the surface but which are highly mobile at the same time, for example amino acids adsorbed onto copper (Szabelski and Sholl 2007b).

To reinforce the importance of the diffusion mechanism, we performed simulations for the same preceding cases but significantly increasing the number of diffusion trials per MC step. The results obtained are shown in Figure 4 which demonstrates the effect of the diffusion on the development of condensate phases, larger that the ones formed when diffusion mechanisms are not stimulated either by temperature or by the algorithm itself.

Finally, to obtain a global view of the appearance of the whole lattice used in our present simulations, we show the amplified versions of Figure 3(a) and Figure 4(b) in Figures 5 and 6, respectively. On comparing the patterns, we again see the intensive effect that diffusion has on the development of condensed phases.

Figure 4. Snapshots of part of the simulated surface for glycine molecules irreversible adsorbed onto the Cu(110) surface. Adsorption energies are the same for the two species. (a) T = 300 K; $W_{22} = W_{11} = -5$ kcal/mol; $W_{21} = W_{12} = +5$ kcal/mol. (b) T = 300 K; $W_{22} = W_{11} = +5$ kcal/mol; $W_{21} = W_{12} = -5$ kcal/mol. (c) The same as for (a) but with T = 800 K. (d) The same as for (b) but with T = 800 K. MC steps $= 5 \times 10^5$ and $N_{diff} = 1 \times 10^7$.
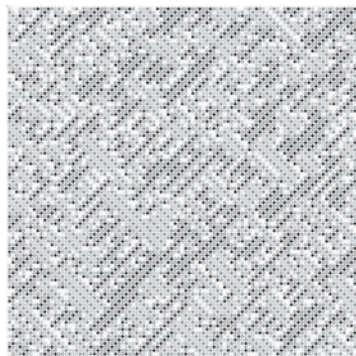
Figure 5. Snapshot of the whole lattice corresponding to the case depicted in Figure 3(a).

Figure 6. Snapshot of the whole lattice corresponding to the case depicted in Figure 4(a).

4. CONCLUSIONS

We have demonstrated in this paper that an adequate set of adsorbate–adsorbate interaction energies can produce ordered phases of homochiral and heterochiral domains. These domains show a notably increase when diffusion increases. The diffusion process can be improved by increasing the temperature or by increasing the number of diffusion trials per Monte Carlo step.

The present model allows the rapid visualization of the ordered surface structures that show up during the adsorption of achiral molecules onto metallic surfaces.

In the context of the present model and the parameters used here, it has been shown that both homo- and hetero-chiral domains cannot be obtained using the same interaction energies at the same time.

This model can be easily extended to the case of energetically heterogeneous surfaces or adsorption energies, depending on the type of footprint.

Finally, and in accordance with Barlow and Raval (2003), we found that the saturated annealed monolayer gives rise to the major ordered phase associated with this organometallic system and

the co-existence of two motifs also results in two possible models for the glycine/Cu(110) superstructure — given in Figures 3(b) and (c) — in which either a homochiral domain containing molecules adsorbed with the same chiral motif is formed, or a heterochiral domain in which both chiral motifs are accommodated is produced.

ACKNOWLEDGEMENTS

REFERENCES

Baiker, A. (1997) *J. Mol. Catal. A* **115,** 473.

Baiker, A. and Blaser, H.U. (1997) in *Handbook of Heterogeneous Catalysis*, Ertl, G., Knözinger, H., Weitkamp, J., Eds, VCH, Weinheim, Germany, Vol. 4, pp. 2422–2436.

Barlow, S.M. and Raval, R. (2003) *Surf. Sci. Rep.* **50,** 201.

Barlow, S.M., Kitching, K.J., Haq, S. and Richardson, N.V. (1998) *Surf. Sci.* **401,** 322.

Barlow, S.M., Louafi, S., Le Roux, D., Williams, J., Muryn, C., Haq, S. and Raval, R. (2004) *Langmuir* **20,** 7171.

Barlow, S.M., Louafi, S., Le Roux, D., Williams, J., Muryn, C., Haq, S. and Raval, R. (2005) *Surf. Sci.* **590,** 243.

Bürgi, T. and Baiker, A. (2000) *J. Catal.* **194,** 445.

Chen, Q., Frankel, D.J. and Richardson, N.V. (2002) *Surf. Sci.* **497,** 37.

Chu, W., LeBlanc, R.J., Williams, C.T., Kubota, J. and Zaera, F. (2003) *J. Phys. Chem. B* **107,** 14 365.

Efstathiou, V. and Woodruff, D.P. (2003) *Surf. Sci.* **531,** 304.

Humblot, V. and Raval, R. (2005) *Appl. Surf. Sci.* **241,** 150.

Humblot, V., Barlow, S.M. and Raval, R. (2004) *Prog. Surf. Sci.* **76,** 1.

Kang, J.-H., Toomes, R.L., Polcik, M., Kittel, M., Hoeft, J.-T., Efstathiou, V., Woodruff, D.P. and Bradshaw, A.M. (2003) *J. Chem. Phys.* **118,** 6059.

Kubota, J. and Zaera, F. (2001) *J. Am. Chem. Soc.* **123,** 11 115.

LeBlond, C., Wang, J., Liu, J., Andrews, A.T. and Sun, Y.K. (1999) *J. Am. Chem. Soc.* **121,** 4920.

Lee, I. and Zaera, F. (2005) *J. Phys. Chem. B* **109,** 12 920.

Lee, I. and Zaera, F. (2006) *J. Am. Chem. Soc.* **128,** 8890.

López, R.H., Romá, F., Gargiulo, V., Sales, J.L. and Zgrablich, G. (2008) *J. Phys. Chem. C*, submitted for publication.

Ma, Z, and Zaera, F. (2005) *J. Phys. Chem. B* **109,** 406.

Mao, L., Harris, H.H. and Stine, K.J. (2002) *J. Chem. Inf. Comput. Sci.* **42,** 1179.

Ortega Lorenzo, M., Haq, S., Bertrams, T., Murray, P., Raval, R. and Baddeley, C. (1999) *J. Phys. Chem. B* **103,** 10 661.

Rankin, R.B. and Sholl, D.S. (2004) *Surf. Sci.* **548,** 301.

Raval, R. (2001) *CATTECH* **5,** 12.

Raval, R. (2002) *J. Phys. Condens. Matter* **14,** 4119.

Raval, R. (2003) *Curr. Opin. Solid State Mater. Sci.* **7,** 67.

Romá, F., Stacchiola, D., Zgrablich, G. and Tysoe, W.T. (2004) *Physica A* **338,** 493.

Romá, F., Zgrablich, G., Stacchiola, D. and Tysoe, W.T. (2003) *J. Chem. Phys.* **118,** 6030.

Rouhi, A.M. (2004) *Chem. Eng. News* **82,** No. 24 (June 14), p. 47.

Stacchiola, D., Burkholder, L. and Tysoe, W.T. (2002) *J. Am. Chem. Soc.* **124,** 8984.

Stacchiola, D., Burkholder, L., Zheng, T., Weinert, M. and Tysoe, W.T. (2005) *J. Phys. Chem. B* **109,** 851.

Szabelski, P. (2004) *Appl. Surf. Sci.* **227,** 94.

Szabelski, P. and Sholl, D.S. (2007a) *J. Phys. Chem. C* **111,** 11 936.

Szabelski, P. and Sholl, D.S. (2007b) *J. Chem. Phys.* **126,** 144 709.

Toomes, R.L., Kang, J.-H., Woodruff, D.P., Polcik, M., Kittel, M. and Hoeft, J.-T. (2003) *Surf. Sci.* **522,** L9.

Tungler, A., Kajtar, M., Mathe, T., Toth, G., Fogassy, E. and Petro, J. (1989) *Catal. Today* **5,** 159.

Uñac, R.O., Gil Rebaza, A.V., Vidales, A.M. and Zgrablich, G. (2007a) *Appl. Surf. Sci.* **25,** 125.

Uñac, R.O., Vidales, A.M., Gargiulo, M.V., Sales, J.L. and Zgrablich, G. (2007b) *Adsorption* **14,** 189.